Experimental Research on Material Behaviour of Glass Fiber Reinforced Polymer Bars in Tension

Wodajo Sara Desalegn [a], Weldeselassie Danayt Abraham [a], Xie Fang [a*], Yang Hongmei [a], Liang Min [a]

[a] School of Civil Engineering, Shaoxing University, Shaoxing 312000, Zhejiang Province, China

sarides21@gmail.com, fangxieusx@163.com

Abstract

Glass Fiber Reinforced Polymer (GFRP) rebars have been widely used to solve the corrosion problem of steel bars in concrete structures. It has been produced as a lightweight and corrosion-resistant than steel reinforcement in many structural applications. They are regarded as a promising substitute for steel bars in concrete infrastructures. It is necessary to test GFRP bars to fully understand their material properties to ensure the safe and efficient use of the material. In this study, five specimens of each type of GFRP bars with a diameter of 6, 8, 10, 12, and 14 mm were tested under tension. Therefore, a total of 25 samples were examined from the same manufacturer. According to ASTM's recommendations (D7205/D7205M-06) for tensile tests of GFRP bars, the diameter and thickness of the steel pipes for both ends were considered in the preparation of the test specimens to keep the GFRP bars consistent and aligned throughout the experiment. The experimental test results included the stress-strain curves, tensile strength, ultimate strain, and modulus of elasticity. The study showed an accurate result that indicated the tensile strength of the GFRP bars can be expressed by a linear distribution. For a bar diameter of 10mm, the length to diameter ratio $L_e/d_b=8$ showed a maximum tensile to compressive strength ratio. In the failure results of the test, there were two-mode failures of GFRP bars: fracture failure and pull-out failure of GFRP bars. Most of the specimens had GFRP bar fracture failures, only two specimens (GBT1-10-2 and GBT1-10-3) were damaged due to the pull-off of the GFRP bars which was not a typical failure mode.

Keywords: *GFRP Bars, Tensile Test, Stress-Strain Curve, Fracture Failure*

1. Introduction

Structural engineers are frequently faced with repairing components of civil infrastructures. Many buildings and highways are structurally deficient, resulting from common problems such as the age of the structure, change in the use of the structure, and deterioration due to environmental exposure. A traditional method of rehabilitating deficient members is steel plate bonding. Over time it was revealed that this method suffered from several disadvantages, such as the difficulty of the installation, the complexity of handling, and the corrosion susceptibility [1]. To solve this problem, an externally bonded fiber-reinforced polymer (FRP) reinforcement is being researched and used to repair and rehabilitate damaged concrete structures as an alternative to the steel plate bonding repair process [1]. FRP bar has several advantages that aid in structural integrity. The composite material is lightweight, non-corrosive, and it is relatively easy to handle. Because FRP bar will be exposed to different types of loads and environments over long periods of service life, the durability of the material must be investigated. The majority of research to date has focused on short-term strengthening without considering the effects of sustained loading and long-term environmental conditions [1]. The durability of concrete structures has always been a great concern. The corrosion of steel reinforcement is one of the most pressing issues in managing durability. Examples of critical structures susceptible to reinforcement corrosion are coastal structures, chemical industry sites, harbors, and bridges. Using an alternate reinforcement material is one solution to this problem. GFRP bars are made of composite fibers and have various distinct characteristics, such as excellent fatigue behavior, high strength to weight ratio, high tensile strength, and non-conductivity [2].

Glass fiber reinforced polymer bars are increasingly used by engineers when designing structures because of their excellent strength properties. This material strength is characterized by its capacity to bear a load without excessive deformation or failure [3]. When a sample of GFRP bar is tested under axial force, the applied force divided by the area of the cross-section (stress) is proportional to the ratio between the change in length and its initial length (strain). GFRP bar gets back to its original shape and length when the applied load is removed. In other words, under axial forces, GFRP bars have linear elastic action [3].

The key mechanical properties governing the structural behaviour of these elements when used as reinforcement in concrete flexural elements are their tensile strength, bond properties, and elastic modulus [2]. GFRP (glass fiber reinforced polymer) composites are now widely used in the manufacturing industries especially in the aircraft, aerospace, and automotive industries due to their outstanding mechanical and thermal properties such as more specific strength, better specific elasticity modulus, high damping factor, or damping capacity, better corrosion resistance, efficient fatigue resistance, and low thermal expansion coefficient. Hence, the machinability behavior of these composites [4] must be understood. Drilling is commonly used in the aforementioned industries to assemble the elements. Because of their isotropic nature and in-homogeneity, the machining of these composites is unlike traditional metals. Fiber pull-out, delamination, and burring of fibers are major disadvantages of these composites in machining. In the machining of GFRP composites, a sufficient set of process parameters is, therefore, an essential concern [4].

The most notable distinctions between GFRP bars and steel-reinforced structures are the significantly low elasticity modulus and the absence of any yield behavior. For a structure, ductility is inelastic energy dissipation that enables internal forces to be redistributed when the structure is near failure, which is typically provided by steel's yield behavior. The GFRP bars themselves cannot be relied upon to provide any ductility, as the bars have limited inelastic energy dissipation due to linear stress-strain behavior before rupture. This implies that to prevent catastrophic failures, failure mechanisms must be carefully considered in GFRP RC design. Ductility must be integrated into the system as a whole, which can be accomplished by introducing redundancy into the framework. In the case of localized failure, a redundant system enables the redistribution of loads. GFRP bars will stretch approximately 20 mm per meter of original length before failure giving a warning by producing large deflections and wide cracks [5].

As creep-rupture is a brittle and unexpected failure mechanism that can occur due to sustained loads exceeding a certain percentage of the ultimate strength, the long-term behavior of GFRP bars must be considered in the design. It is widely accepted that a GFRP RC section would need to be over-reinforced for most structural applications, which corresponds to a reinforcement ratio greater than about 0.5 percent (fib 2007) for GFRP bars [6]. Currently, there is no standardized procedure for GFRP bar manufacture, so there can be significant variations in the properties of 'similar' products from different manufacturers [5].

Subsequently, global output grew exponentially hitting the current development in the late 1960s [7]. The combination of low material, manufacturing costs, and developments in member manufacturing rendered polymer production to be cost-effective and disseminated to other fields. Furthermore, due to its outstanding manufacturing adaptability, high resilience, and structural performance (strength-to-weight ratio), GFRP bars offer very versatile design solutions and benefit from increasingly low production and erection costs [8,9,10,11].

The process of producing composite materials by mixing two different materials is not new. Ancient Egyptians used a straw to strengthen mud to create a stronger composite material. Only a later version of this concept is the fiber-reinforced polymer. The use of Fiber Reinforced Polymer (FRP) bars goes back to the 1950s after World War II in various fields such as the aerospace and automotive industries. Nowadays different parts of today's vehicles are made of composites. Many large parts of modern aircraft are made out of composites as they are lighter and more fatigue resistant compared to traditional materials [12].

Benmokrane et al. (2000) [13], tested four different types of FRP bars in tension using a similar test setup to ASTM D7205/7205M-06 [14]. The tested specimens they used had a length of 1600 mm and were embedded in 600 mm steel anchors that had an inner diameter of 30 mm that was grouted with high-performance resin grout. At the end of the test, they were able to achieve failure in the free length indicating that the test can be used to determine the ultimate tensile strength of the bars.

Arczewska P., Polak M.A., and Penlidis A. (2019) [15] tested the determination of tensile characteristics of GFRP bars including the tensile strength, ultimate strain, and elasticity modulus according to different test standards. Test results for tensile characterization were obtained on four types of GFRP bars from four manufacturers with six different diameters. Besides, according to seven criteria, the analysis contrasts different test procedures to describe the tensile properties of GFRP bars to analyze the proposed test procedures and to expose the key differences.

The overall objective of the study is to define and assess the overall adequacy of the use of GFRP reinforcing products as a substitute for reinforced concrete steel reinforcement. Due to a lack of information about the actions of such participants, the efficient use of GFRP reinforcement in deep members has been hindered. To date, most studies have concentrated primarily on the flexural or shear behavior of longitudinally reinforced shallow members with GFRP and most of them used small-scale research. Therefore, this study aims to provide

engineers and researchers with a better understanding of the analysis and behavior of tensile GFRP reinforced members. The results obtained throughout this study characterize the tensile behavior of GFRP bars and present an experimental study to examine the proposed test method that addresses the issues.

2. Experimental Behavior

Overall, this test method presents a GFRP bar embedded at the end using adhesive anchors and steel caps, to be tested consistently under tensile load until it fails in a mechanical testing machine. The aim of developing this test method was to assist researchers and designers in assessing tensile strength, elasticity modulus, and stress-strain curve. The gripping and alignment are performed during the test specimen preparation process. By confining the ends of GFRP bars, the steel cap and adhesive anchors act as a gripping method to prevent premature failure and allow them to obtain their maximum tensile capacity. Besides, when the adhesive anchors are mounted, the alignment can simply be carried out, which can prevent unnecessary bending and premature failure and improve the accuracy of test results. For each test condition, testing five specimens is recommended to record clear and agreed data sets.

Steel cap, plastic cover, rivet, and adhesive anchors are among the components of the test fixture. It is suggested that the diameter of the steel cap be considered twice the effective bar diameter, although its length is recommended to be the same as the effective bar diameter. The steel cap must be dense enough not to be yielded or distorted by the adhesive anchor lateral strain. To give a free length equal to twice its diameter, the steel cap should be connected to a plastic cover with a square cross-section.

The process starts with the preparation of specimens by preparing steel caps, then setting up GFRP bars for the first end of the specimen while monitoring the orientation, and ending with doing the same for the other end. Fully smooth and perpendicular to its longitudinal axis must be the ends of the GFRP bar. It is important to check the orientation of the specimen if it is positioned in the center and perpendicular to it. After positioning the GFRP bar at the center of the steel cap, insert the rivets into the steel cap and add adhesives to it. If the preparation is finished, by applying a uniform and monotonic tension force, the specimens can be examined. If no premature cap failure is detected, the test results are deemed appropriate. In other words, if the breakage of GFRP bars occurs at the free length of the specimen, the experiments are completed successfully.
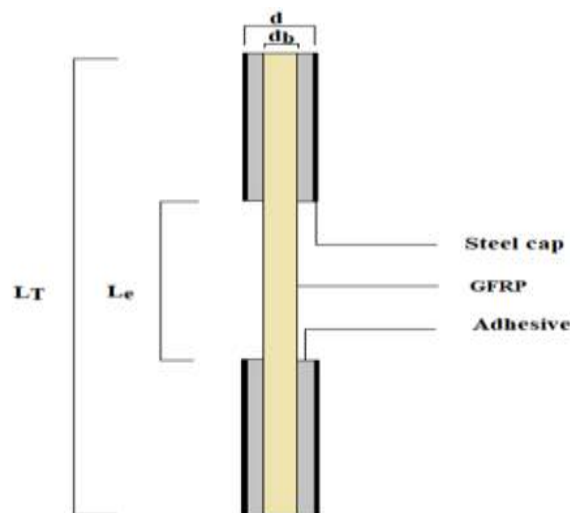

Figure 1. The physical picture of the GFRP tendon.

2.1 Test Plan

The tensile properties of GFRP bars of five different diameters have been evaluated in this test and the effect of the diameter on the tensile properties of GFRP bars has been analyzed. To ensure the reliability of the test results, a total of five groups having 25 test pieces were analyzed for 5 test pieces in each group.

Table 1. Tensile specimen grouping.

D (mm)	L$_T$ (mm)	L$_e$ (mm)	Quantity
6	1000	400	5
8	1000	400	5
10	1000	400	5
12	1000	400	5
14	1000	400	5

D= Diameter; L$_T$= Total Length; L$_e$=Effective Length

2.2 Test Materials

2.2.1 GFRP bars

The GFRP bar developed by Zhejiang Xinna Composite Material Co., Ltd. with diameters of 6, 8, 10, 12, and 14mm is the material used in this test. Due to the high demand for building infrastructure, these bars were chosen. Figure 2 demonstrates the physical image of the tensile test piece.

Figure 2. The physical picture of GFRP tendons.

2.2.2 Adhesives (504AB Glue)

According to GB/T 30022-2013 specification, make a GFRP tendon test piece. During the manufacturing process, first put one end of the galvanized steel pipe. Seal, then pour 504AB glue on the other end until it is about to overflow, and then insert the GFRP tendon into the tube and center it. Consider the adhesion between the steel pipe and the 504AB glue that may not be enough. Insert 4 rivets in advance at the end where the steel pipe is sealed. In this way, it improves the adhesion between the steel pipe and the glue which enables the GFRP tendons to be better centered.

Figure 3. The physical picture of 504AB Glue.

Table 2. GFRP tendon design matrix.

No.	Material	Specification	Quantity
1	Galvanized steel pipe	thickness 2mm, length 300mm	50
2	504AB glue	-	40
3	Rivet	length 50mm, thickness 3mm	200

2.2.3 Steel cap

The functions of the steel cap are holding the GFRP bar, alignment, gripping action, and strengthening the ends

of the specimens. The ease of alignment and gripping are the advantages of using the steel cap filled with high strength and fast setting anchoring adhesive. The alignment is controlled once GFRP is inserted into the steel cap filled with adhesives to align the GFRP bar and steel cap. It is necessary to cut the ends of the GFRP bars perpendicular to the longitudinal axis of the bars and to place the bars at the center of the steel caps. Then, a level at the flat surface of the GFRP bar can give the required alignment. For the second steel cap, the process should be repeated once the adhesive is fixed. The steel caps offered a solid capping for the GFRP bar after the adhesive was set, to avoid any premature crushing at the ends. The lateral containment of the steel rings filled with an adhesive provided by the end of the GFRP bar helps to prevent localized crushing of the ends of the GFRP bar.

Figure 4. The physical picture of a steel cap.

2.2.4 Rivet

Mechanical fasteners such as rivets or bolts are also used to fasten GFRP laminates. A rivet is a mechanical fastener composed of a head on one end and a cylindrical stem on another (called the tail) which has the appearance of a metal pin. They won't loosen when subjected to vibration and can secure joints with short clamp lengths. Choosing the correct size of the rivet while mounting makes the test samples vibration-resistant and permanent.

Figure 5. The Physical Picture of a Steel Cap.

2.2.5 Plastic cover

The plastic cover used during sample fabrication was a PVC material which prevented the adhesive material from pouring out of both ends of the specimens. It was placed on both the top and bottom of the specimen by using 502 super glue.

(a) Plastic cover   (b) 502 super glue   (c) Steel cap

Figure 6. Placement of plastic cover on both ends of the steel cap.

2.3 Test scheme and sample preparation

In this study, GFRP bars with five different diameters of 6, 8, 10, 12, and 14 mm were prepared, with a total length of 1000 mm. The length of the GFRP test piece includes the anchor length of 300 mm at both ends and the effective length of 400 mm in the middle for all specimens. The geometric dimensions and schematic diagram of GFRP bars are shown in Figure 7.
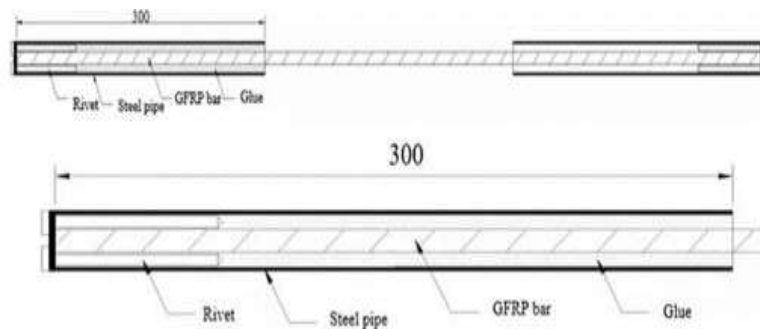

Figure 7. Schematic Drawing of GFRP Bar.

Figure 8. A Physical Sampling of GFRP Bar.

The specimens for the tensile test were prepared according to the ASTM D7205 [16] guidelines. The total length (L_T) of the tensile specimen was 1000mm. The free length between the steel tube anchors (L_e) was 400mm. A steel tube with an outside diameter d of 21mm, inside diameter d_b of 19mm, and seamless length of 300mm. The epoxy resin and hardener were used to fill the void between the bars and the steel tubes. For proper alignment, the steel tubes and bars were mounted vertically in a wooden frame. The first anchor was turned upside down after 72 hours and the same process for the second anchor was repeated. According to the requirements given by the resin manufacturers, in standard indoor laboratory conditions, the total setting time for both sample anchors was 72 hours.

2.3.1 Test Equipment and Loading Scheme

The overall prepared specimens of GFRP bars were conducted by utilizing the 1000 kN electro-hydraulic servo universal testing machine under tension loading. The loading method adopts displacement loading and a loading rate of 5mm/min. The relation between the load and displacement was linear until an abrupt drop in the load occurred indicating the occurrence of failure without showing any plateau or any kind of ductile behavior. The test samples showed brittle behavior. As shown in Figure 9, the data was collected with effective gauge length and GFRP tendons for different diameters were used for the tensile test.

Figure 9. Laboratory Tensile Strength Test Machine

3. Test Results

3.1 Failure Modes

In the failure results of this test, GFRP tendons have two failure modes: tensile failure of GFRP tendons and pull-off failure of GFRP tendons.

3.1.1 GFRP Tendons Pulled-off Failure

In this test result, only two test pieces with a diameter of 10 mm were damaged due to the pull-off of the GFRP rib ends. The samples were GBT1-10-2 and GBT1-10-3, as shown in Figure 10.

Figure 10. GFRP tendons at the end of the pull-off failure

3.1.2 GFRP Tendons Fracture Failure

Among the failure specimens obtained in this test, most specimens had GFRP tendon fracture failure, as shown in Figure 11. Most of the failure mechanisms found from the tension test were performed as defined by the fracture of the fibres in the free length of the bars. Besides, the form of failure was a brittle type of failure as predicted where the breakage of the free-length fibres occurred suddenly without any yield.

Figure 11. GFRP tendon fracture failure diagram

3.2 Calculation of Tensile characteristics

The tensile test was conducted using a universal testing machine with a capacity of 600kN at the strength of the materials laboratory. The loading rate was at 5mm/min until the failure of the tensile specimen. The ultimate load, tensile strength, elastic modulus, and ultimate strain of GFRP bars obtained in this test are shown in Table 4. Overall, these tests showed a slightly higher modulus of elasticity in compression and tension, by comparing the results of compressive to tensile tests. However, if the guaranteed tensile characteristics of bars reported by the manufacturer are used for the sake of comparison.

3.2.1 Tensile strength

It varies with the cross-sectional dimensions of the bar due to the shear lag effect and therefore tensile strength should be referenced based on the bar size. To determine the tensile strength, the tensile strength of GFRP bar samples was determined according to Equation 1.

$$f_{ft} = \frac{F_t}{A} = \frac{4F_t}{\pi d^2} \tag{1}$$

Where f_{ft} is tensile strength in MPa; F_t is the tensile ultimate load value of the test piece in N; d is the diameter of the test piece in mm.

Table 3. Details of tension test specimens.

No.	Specimen No.	D (mm)	A (mm²)	L_T (mm)	Le (mm)
1	GBT1-6-1	6.00	28.27	1000	400
2	GBT1-6-2	6.00	28.27	1000	400
3	GBT1-6-3	6.00	28.27	1000	400
4	GBT1-6-4	6.00	28.27	1000	400
5	GBT1-6-5	6.00	28.27	1000	400
6	GBT1-8-1	8.00	50.27	1000	400
7	GBT1-8-2	8.00	50.27	1000	400
`8	GBT1-8-3	8.00	50.27	1000	400
9	GBT1-8-4	8.00	50.27	1000	400
10	GBT1-8-5	8.00	50.27	1000	400
11	GBT1-10-1	10.00	78.54	1000	400
12	GBT1-10-2	10.00	78.54	1000	400
13	GBT1-10-3	10.00	78.54	1000	400
14	GBT1-10-4	10.00	78.54	1000	400
15	GBT1-10-5	10.00	78.54	1000	400
16	GBT1-12-1	12.00	113.10	1000	400
17	GBT1-12-2	12.00	113.10	1000	400
18	GBT1-12-3	12.00	113.10	1000	400
19	GBT1-12-4	12.00	113.10	1000	400
20	GBT1-12-5	12.00	113.10	1000	400
21	GBT1-14-1	14.00	153.90	1000	400
22	GBT1-14-2	14.00	153.90	1000	400
23	GBT1-14-3	14.00	153.90	1000	400
24	GBT1-14-4	14.00	153.90	1000	400
25	GBT1-14-5	14.00	153.90	1000	400

D=Diameter; A=Area; L_T=Total length; L_e=Effective length

3.2.2 Ultimate strain

It is the strain that is corresponding to the maximum stress point on the stress-strain curve, and the material will fail after reaching this point. The ultimate strain of GFRP bar samples was determined according to Equation 2.

$$\varepsilon_t = \frac{F_t}{E_{ft}A} \tag{2}$$

Where Ft is the tensile ultimate load value of the test piece in N; Eft is the tensile elastic modulus in GPa; A is the cross-sectional area of the test piece in mm².

3.2.3 Modulus of elasticity

It is the slope of load–strain curve obtained from an extensometer or strain gauge readings. Equation 3 is used to calculate the value of the modulus of elasticity:

$$E_{ft} = \Delta \sigma_t / \Delta \varepsilon_t \tag{3}$$

Where, $\Delta \sigma_t$ is the difference in applied tensile stress between the starting and ending points in MPa; $\Delta \varepsilon_t$ is the difference in tensile strain between the starting and ending points in %.

Table 4. GFRP Tensile Test Result

No.	Specimen No.	D (mm)	F_t (kN)	f_{tu} (MPa)	E (Gpa)	ε (%)
1	GBT1-6-1	6.00	40.46	1431	58.50	0.0244
2	GBT1-6-2	6.00	44.58	1577	58.03	0.027
3	GBT1-6-3	6.00	41.61	1472	56.62	0.026
4	GBT1-6-4	6.00	42.88	1517	57.64	0.026
5	GBT1-6-5	6.00	38.16	1350	57.87	0.023
6	GBT1-8-1	8.00	69.76	1388	57.34	0.024
7	GBT1-8-2	8.00	63.45	1262	57.54	0.022
8	GBT1-8-3	8.00	68.08	1354	58.10	0.023
9	GBT1-8-4	8.00	67.06	1334	58.02	0.023
10	GBT1-8-5	8.00	66.46	1322	58.14	0.023
11	GBT1-10-1	10.00	113.78	1449	60.77	0.024
12	GBT1-10-2	10.00	85.18	1085	60.64	0.018
13	GBT1-10-3	10.00	90.70	1155	60.09	0.019
14	GBT1-10-4	10.00	113.08	1440	61.36	0.023
15	GBT1-10-5	10.00	112.62	1434	61.32	0.023
16	GBT1-12-1	12.00	136.11	1203	52.63	0.023
17	GBT1-12-2	12.00	139.56	1234	53.06	0.023
18	GBT1-12-3	12.00	151.65	1341	53.22	0.025
19	GBT1-12-4	12.00	150.89	1334	54.76	2.436
20	GBT1-12-5	12.00	151.12	1336	55.49	2.408
21	GBT1-14-1	14.00	199.97	1299	52.39	2.479
22	GBT1-14-2	14.00	196.40	1276	52.65	2.424
23	GBT1-14-3	14.00	195.66	1271	52.69	2.412
24	GBT1-14-4	14.00	195.98	1273	53.32	2.387
25	GBT1-14-5	14.00	205.12	1333	53.01	2.515

D=Diameter; F_t=Ultimate load; f_{tu}=Tensile strength; E=Elastic modulus; ε=Ultimate strain

3.3 Stress-Strain Curves

A stress-strain curve is a graphical representation of the behaviour of a material when it's subjected to a load or force. The two characteristics that are plotted are stress on the *y*-axis and strain on the *x*-axis. Stress is the ratio of the load or force to the cross-sectional area of the material to which the load is applied. The standard units of measure for stress are pounds per square inch or Newtons per meter squared. Strain, on the other hand, is a measure of the deformation of the material as a result of the force applied. Deformation is a change in the shape or form of the material.
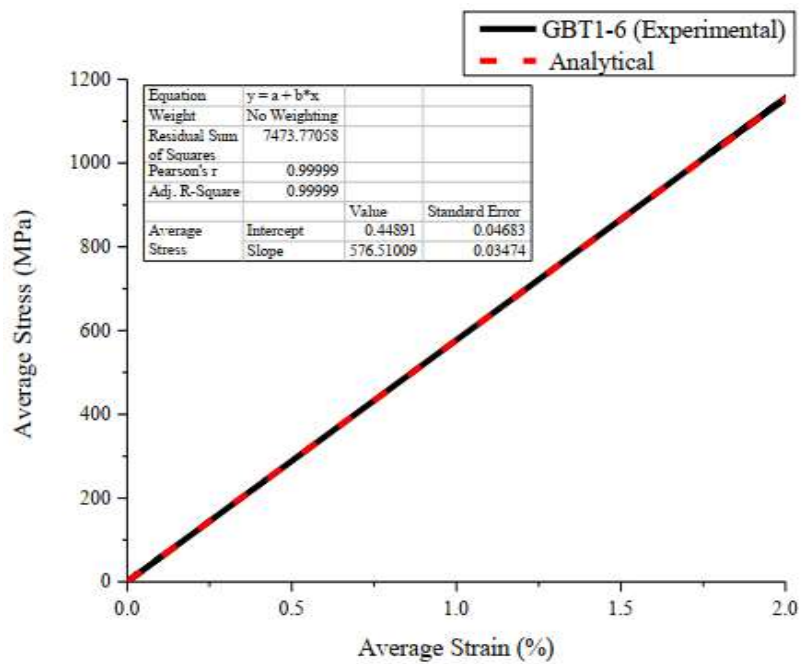
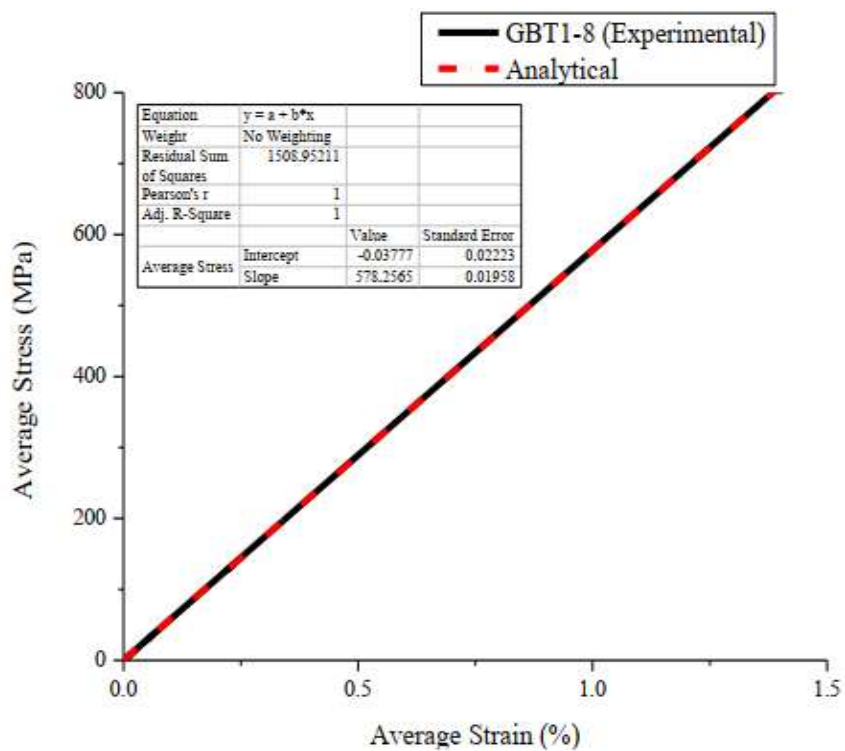**Figure 11.** Average Stress-Strain curve of GBT1-6 specimen

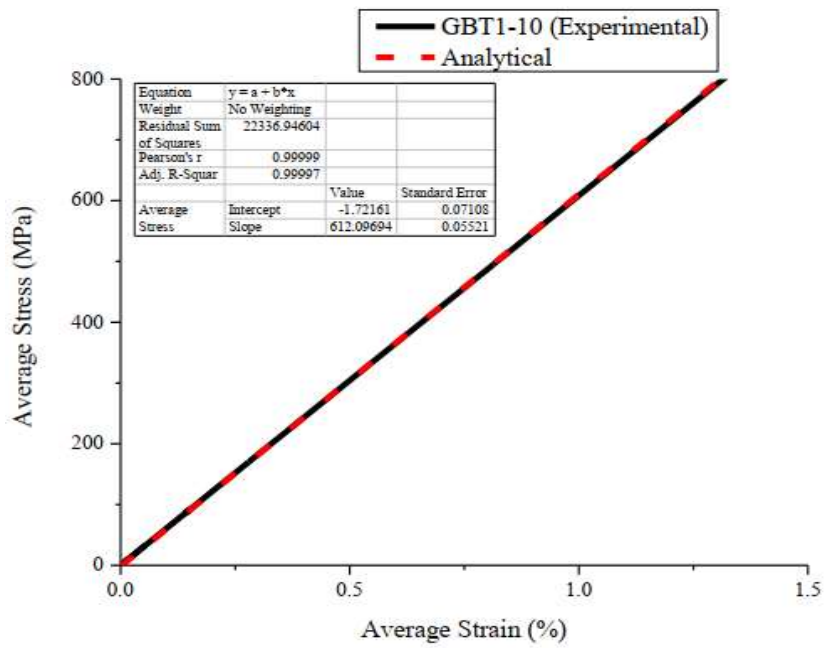**Figure 12.** Average Stress-Strain curve of GBT1-8 specimen

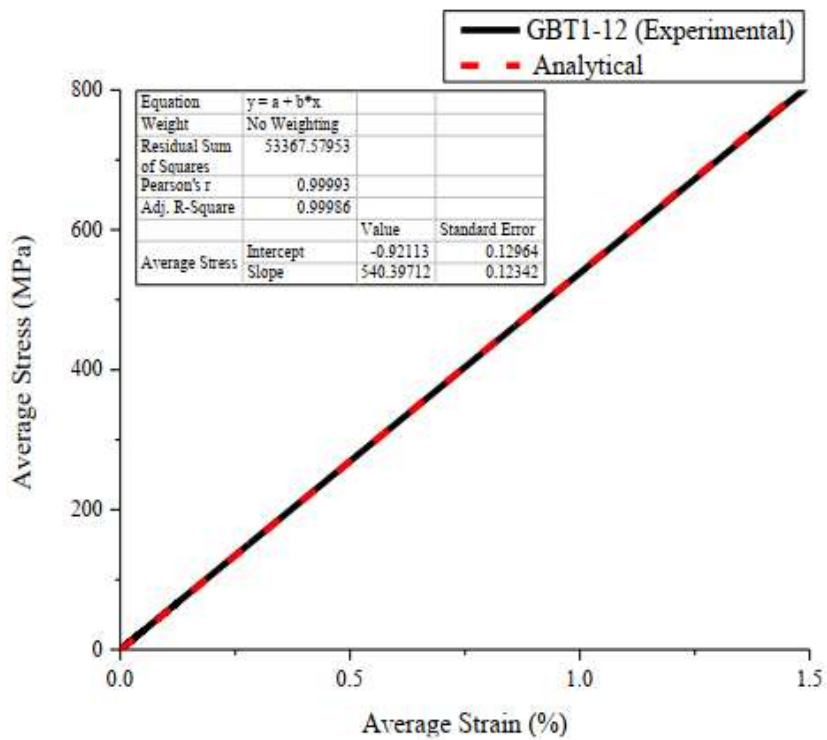**Figure 13.** Average Stress-Strain curve of GBT1-10 specimen

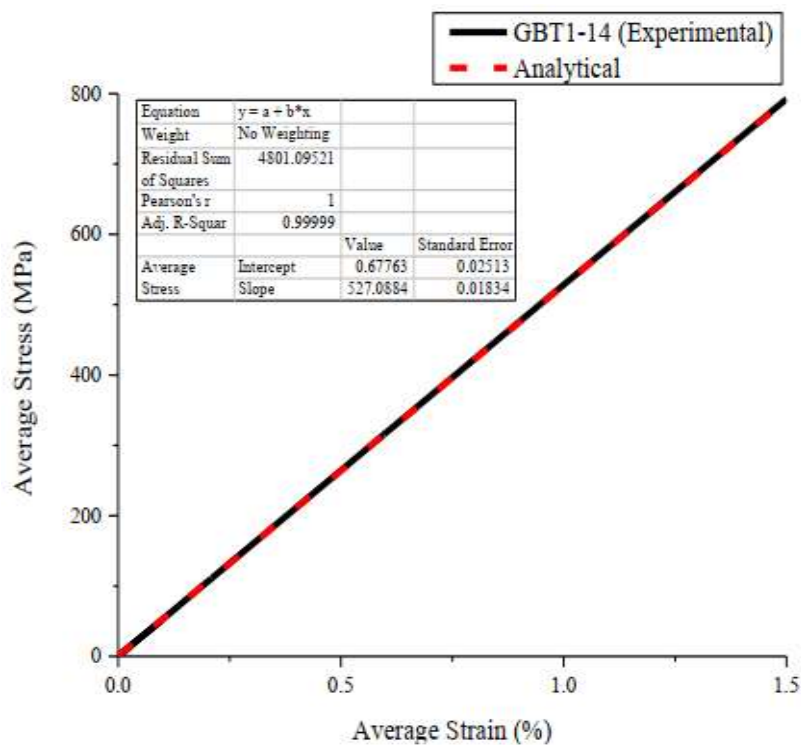**Figure 14.** Average Stress-Strain curve of GBT1-12 specimen

Equation	y = a + b*x		
Weight	No Weighting		
Residual Sum of Squares	4801.09521		
Pearson's r	1		
Adj. R-Squar	0.99999		
		Value	Standard Error
Average Stress	Intercept	0.67763	0.02513
	Slope	527.0884	0.01834

Figure 15. Average Stress-Strain curve of GBT1-14 specimen

Table 5 Comparison of GFRP bars based on Average Stress-Strain value

Bar size	6	8	10	12	14
Error	0.046	**0.022**	0.071	0.129	0.025
R^2	0.999	**1**	0.997	0.986	0.999

R^2= Regression

Based on the test results and analysis, it was found that the most representative value for the stress-strain data was bar diameter 8mm. The standard error of this sample was relatively the smallest having a regression (R^2) value of 1. Therefore, when the value of the standard error becomes smaller, the value of regression (R^2) approaches 1 which enables the curve to be more linear.

4. Characteristics of GFRP bars under different load modes

4.1 Characteristics under Ultimate Load

Based on the test results and analysis, it was found that the most representative value for the average ultimate load data was bar diameter 14mm. As the diameter of the GFRP bar increased, the ultimate load also increased.

Table 6. Average Ultimate Load versus Diameter

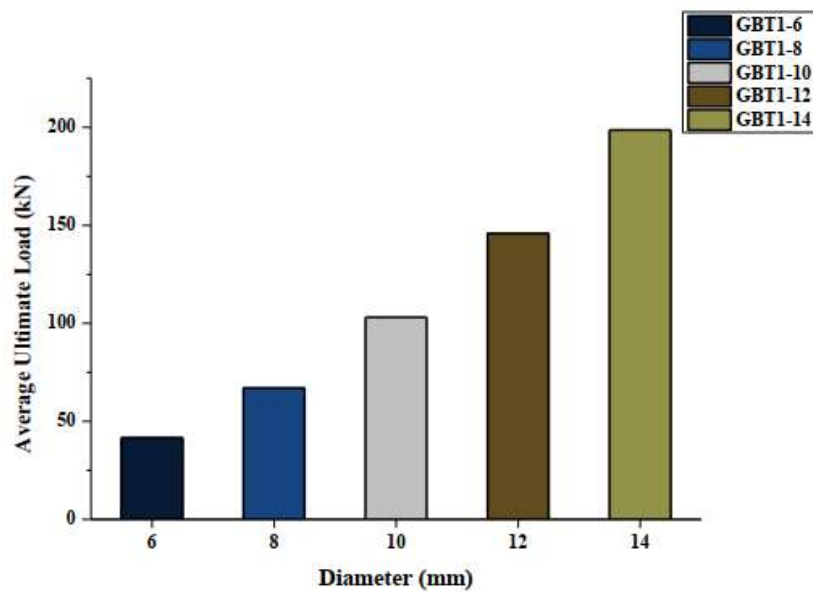| Bar size	6	8	10	12	14
Ultimate Load (kN)	41	67	103	146	199

Figure 16. Average Ultimate Load versus Diameter.

4.2 Characteristics under Tensile Strength

Based on the test results and analysis, it was found that the most representative value for the average tensile strength data was bar diameter 10mm. As the diameter of GFRP bars increased, the tensile strength decreased. Bar diameter 6mm has attained the maximum tensile strength but since it's not recommended for construction by considering the elastic modulus of the bars, the bar diameter 10mm was chosen

Table 7. Comparison of GFRP bars based on Average Tensile Strength versus Diameter

Bar size	6	8	10	12	14
Tensile Strength (MPa)	1469	1332	1312	1290	1290
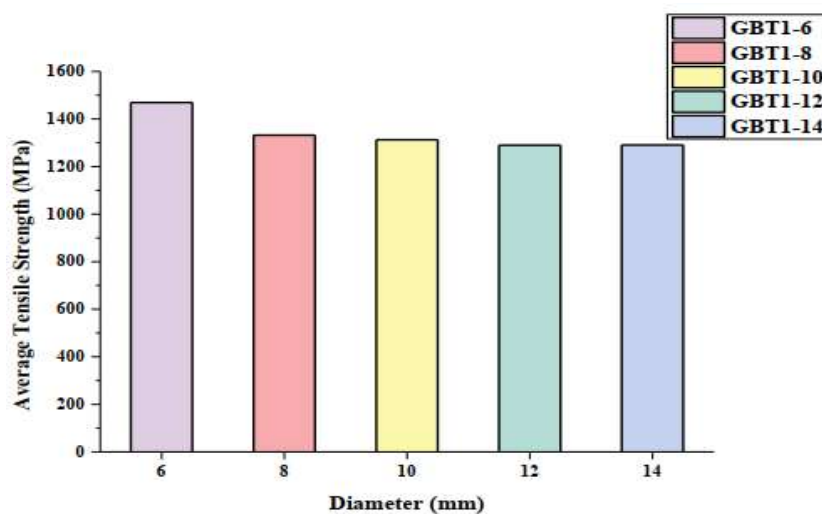
Figure 17. Average Tensile Strength versus Diameter.

4.3 Characteristics under Elastic Modulus

Based on the test results and analysis, it was found that the most representative value for the average elastic modulus was bar diameter 10mm. The elastic modulus of GFRP bars increased from 6mm to 10mm and decreased from bar 10mm to bar 14mm. The modulus of elasticity was calculated as the slope of the linear elastic part of the stress and strain curve. Similar to the method proposed by ASTM D7205/D7205M for the determination of the GFRP bar elasticity tensile modulus, the GFRP bar elasticity modulus was determined from the slope of the linear lines between 1000 μe and 3000 μe.

Table 8. Comparison of GFRP bars based on Average Elastic Modulus versus Diameter

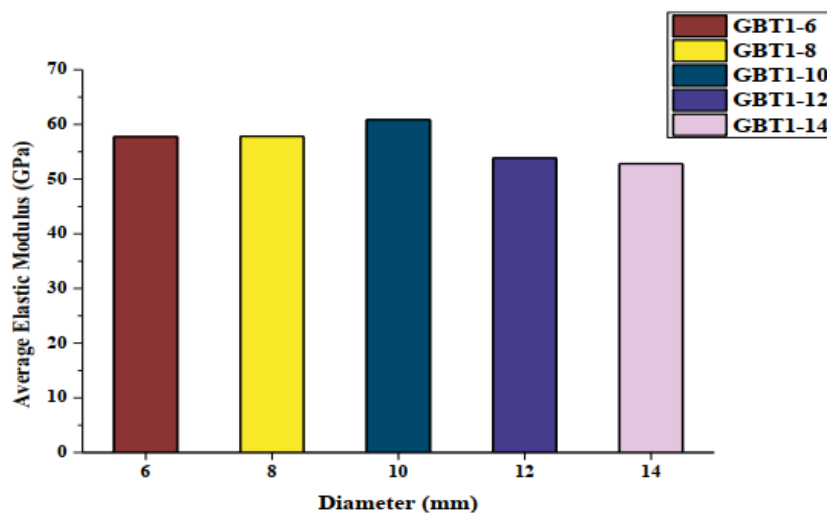| Bar size	6	8	10	12	14
Elastic Modulus (Gpa)	58	58	61	54	53

Figure 18. Average Elastic Modulus versus Diameter.

4.4 Characteristics under Ultimate Strain

Based on the test results and analysis, it was found that the most representative value for the average ultimate strain data was bar diameter 10mm. The ultimate strain decreased from bar diameter 6m to 10mm and increased from the bar diameter 10mm to 14mm.

Table 9. Comparison of GFRP bars based on Average Ultimate Strain versus Diameter

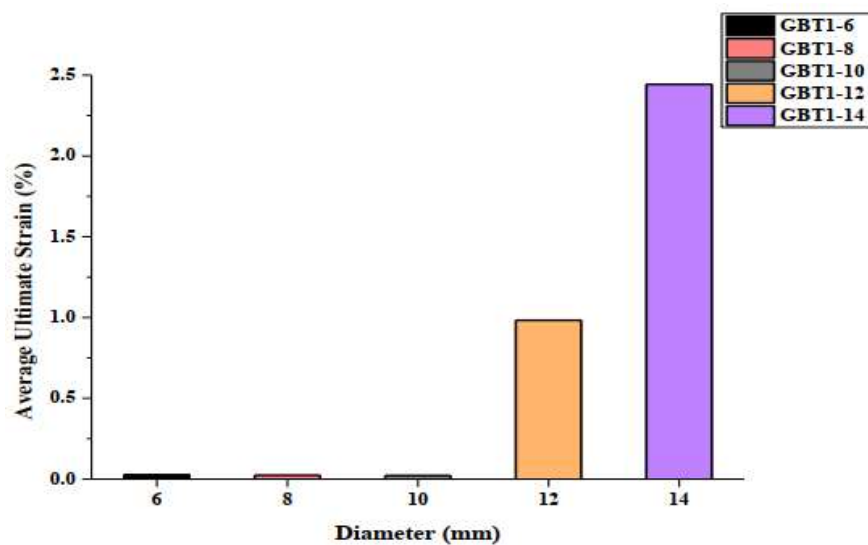| Bar size	6	8	10	12	14
Ultimate Strain	0.025	0.023	0.0214	0.983	2.44

Figure 19. Average Ultimate Strain versus Diameter

5. Compressive Mechanical Properties of GFRP Bars

In the test, a total of 27 specimens were tested for the proposed test procedure. The diameter of the GFRP tendon used in the test was 10, 12, and 14 mm, and the effective length to bar diameter ratio Le/db (4, 8, and 16) was investigated for the compressive strength of the bars. The lengths of the specimens were varied to establish the relationship between length and strength. Besides, two steel caps with a length of 50 mm each were installed to both ends of each specimen to avoid premature failure. It was observed that the test method enables to successfully evaluate the compressive characteristics of the GFRP bars. In this study, there will be a comparison of tension with compression test results by conducting a tensile to compressive ratio.

5.1 Characteristics under Tensile to compressive strength and modulus ratio

The average compressive modulus of elasticity and strength of each slenderness ratio (L_e/d_b ratio) of GFRP bars are presented in Table 11. It was seen that the average modulus of elasticity in compression and tension have differences, and the average strength of tension is 75.36% higher than compressive strength when compared to the slenderness ratio of 8 for bar diameter 10 mm. The tensile to compressive strength and modulus of elasticity ratios for the tested groups is presented in Figure 20 and 21, respectively. It was observed that the modulus of elasticity in compression is higher than tension when comparing with the slenderness ratio of 8 for bar diameter 10 and 12 mm by 1.42% and 13.3%, respectively. It shows that the modulus of elasticity of GFRP bars in compression can be considered the same as in tension. However, for determining the compressive strength, the compressive test is necessary due to the wide variety of compressive to tensile strength ratios. In other words, the test of GFRP bars in tensile is not sufficient to estimate the compressive strength of the GFRP bars.

Table 10. Average Tensile test results of the GFRP bars.

D (mm)	f_{ft} (MPa)	E_{ft} (GPa)	εt (%)	SD	CoV
6	1469.4	57.732	0.0253	86	5.6
8	1332	57.83	0.023	46.43	3.5
10	1312.6	60.836	0.0214	177.63	13.53
12	1289.6	53.832	0.983	65.87	5.11
14	1290.4	52.812	2.44	26.34	2.04

D= Diameter f_{ft} =Ultimate tensile strength; E_{ft}=Tensile modulus of elasticity; εt=Ultimate tensile strain; SD= Standard deviation; CoV= Coefficient of variance.
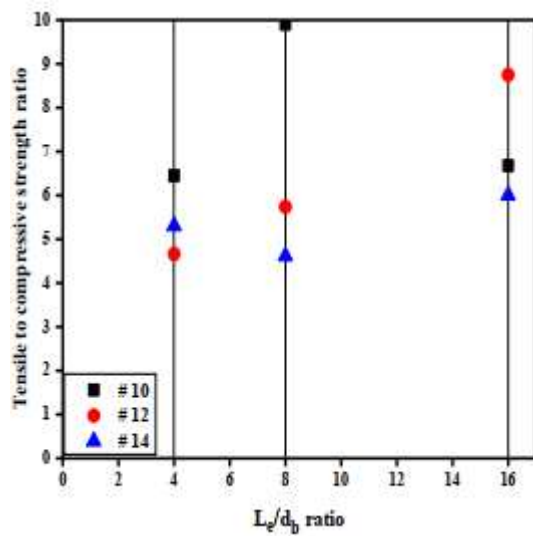
Figure 20. Tensile to compressive strength ratio versus slenderness ratio (Le/db ratio).
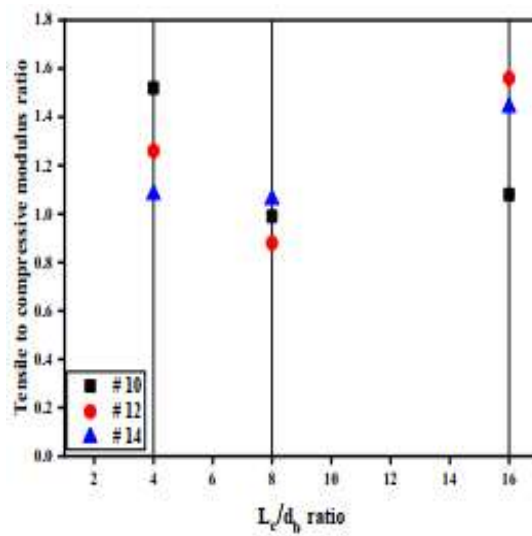

Figure 21. Tensile to compressive modulus ratio versus slenderness ratio (Le/db ratio).

Table 11. Tensile to compressive strength (MPa) and modulus (GPa) ratios of the tested GFRP bars with various L_e/d_b.

Sample No.	10 mm bar L_e/d_b ratio			12 mm bar L_e/d_b ratio			14 mm bar L_e/d_b ratio		
	4	8	16	4	8	16	4	8	16
A	200.53	341.33	192.38	274.90	219.71	118.45	237.07	263.59	215.92
B	-	307.38	186.81	-	234.06	173.88	249.62	296.40	225.66
C	205.98	-	210.02	278.2	220.48	149.85	-	-	204.07
$f_{fc\ avg}$	203.26	323.36	196.40	276.55	224.75	147.39	243.35	280	215.22
$E_{fc\ avg}$	40	61.71	56.60	42.73	60.98	34.57	48.91	49.83	36.54
$(f_{ft}/f_{fc})_{avg}$	6.45	9.9	6.68	4.66	5.74	8.75	5.30	4.61	6
$(E_{ft}/E_{fc})_{avg}$	1.52	0.99	1.08	1.26	0.88	1.56	1.08	1.06	1.44

Note: $E_{ft\ avg}$ = average tensile modulus of elasticity of GFRP bars; f_{ft} = tensile strength of GFRP bars; $E_{fc\ avg}$ = average compressive modulus of elasticity of GFRP bars; $f_{fc\ avg}$ = average compressive strength of GFRP bars.

6. Conclusion

By undertaking an experimental program involving twenty-five GFRP bar specimens concentrically loaded up to failure, this research attempted to comprehensively and systematically investigate the tensile mechanical characteristics of GFRP rebars. Using the experimental method, the influence of the bar diameter and effective length on the tensile behaviour of GFRP bars was observed. The following conclusion is drawn based on the test results and observations:

1. A reliable and consistent tensile strength of GFRP bars was allocated to the proposed new method of testing the GFRP bars under tension. This method made it easier to position the specimens longitudinally upright and concentrate the tensile loads without causing premature failure in the tested bars.

2. The GFRP bars of 10 mm diameter have the most representative value for tensile strength and elastic modulus and are recommended for tension testing of GFRP bars. The diameter of the bar influences the failure mode of the GFRP bars of the same effective length. GFRP tendon fracture failure appeared in most specimens. Only two test samples (GBT1-10-2 and GBT1-10-3) were damaged due to the pull-off of the GFRP rib ends due to improper sample preparation.

3. The difference between the measured tensile strength of GFRP bars with different bar diameters was slight. The average tensile strength of GFRP bar specimens decreased from 6 mm to 14 mm in bar diameter. The average elastic modulus of GFRP bar specimens increased from 6 mm to 10 mm in bar diameter and

decreased from 10 mm to 14 mm in bar diameter. Therefore, by taking into account both the average elastic modulus and tensile strength, 10 mm is the most representative bar diameter.

4. Bars with smaller diameters are more effective than larger ones when resisting tensile loads.

5. It was observed that a good assumption was to consider a linear behavior for the tensile stress-strain curves of GFRP bars.

6. For a bar diameter of 10 mm, the standard deviation and coefficient of variance of the tensile strength test results are higher with 177.63 and 13.53%, respectively.

7. For a bar diameter of 10 mm, the average tensile strength of the GFRP bar was 75.53% higher than its average compressive strength with a L_e/d_b ratio of 8.

8. The average compressive modulus of elasticity of L_e/d_b ratio of 8 is higher than the tensile strength of bar diameter 10 and 12 mm by 1.42% and 13.3%, respectively.

Declaration

References

[1] Chajes, M. J., Finch, W. W., & Thomson, T. A. (1996). Bond and force transfer of composite-material Plates bonded to concrete. *Structural Journal*, *93*(2), 209-217.

[2] Benmokrane, B., Wang, P., Ton-That, T. M., Rahman, H., & Robert, J. F. (2002). The durability of glass fiber-reinforced polymer reinforcing bars in a concrete environment. *Journal of Composites for Construction*, *6*(3), 143-153.

[3] Deitz, D. H., Harik, I. E., & Gesund, H. (2003). Physical properties of glass fibre reinforced polymer rebars in compression. *Journal of Composites for Construction*, *7*(4), 363-366.

[4] Sahu, S. K. (2015). *Drilling of Glass Fiber Reinforced Polymer (GFRP) Composites: Multi Response Optimization Using Grey Relation Analysis with Taguchi's Method* (Doctoral dissertation).

[5] Micelli, F., & Nanni, A. (2004). The durability of FRP rods for concrete structures. *Construction and Building materials*, *18*(7), 491-503.

[6] Nishizaki, I., & Meiarashi, S. (2002). Long-term deterioration of GFRP in water and moist Environment. *Journal of composites for construction*, *6*(1), 21-27.

[7] Vijay, P. V., & GangaRao, H. V. S. (1999). Accelerated and natural weathering of glass fiber reinforced Plastic bars. *Special Publication*, *188*, 605-614.

[8] Debaiky, A. S., Nkurunziza, G., Benmokrane, B., & Cousin, P. (2006). Residual tensile properties of GFRP reinforcing bars after loading in severe environments. *Journal of Composites for Construction*, *10*(5), 370-380.

[9] Karbhari, V. M., Murphy, K., & Zhang, S. (2002). Effect of concrete-based alkali solutions on Short-term durability of E-glass/vinyl ester composites. *Journal of Composite materials*, *36*(17), 2101-2121.

[10] Karbhari, V. M., Stachowski, C., & Wu, L. (2007). The durability of pultruded E-glass/vinyl ester Under combined hygrothermal exposure and sustained bending. *Journal of materials in civil engineering, 19(8), 665-673.*

[11] Porter, M. L., & Barnes, B. A. (1998, January). Accelerated aging degradation of glass fiber Composites. In *Second International Conference on Composites in Infrastructure National Science Foundation* (Vol. 2).

[12] Nanni, A., Composites: coming on strong Concrete Construction, 1999. 44(1): p. 120-124.

[13] Benmokrane, B., Zhang, B., & Chennouf, A. (2000). Tensile properties and pull out behavior of AFRP and CFRP rods for grouted anchor applications. *Construction and Building Materials*, *14*(3), 157-170.

[14] ASTM Standard D7205/7205M-06, "Standard Test Method for Tensile Properties of Fiber Reinforced Polymer Matrix Composite Bars", ASTM International, West Conshohocken, PA. (2016). DOI:10.1520/D7205_D7205M-06R16.

[15] Arczewska, P., Polak, M. A., & Penlidis, A. (2019). The relation between tensile strength and modulus of rupture for GFRP reinforcing bars. *Journal of Materials in Civil Engineering*, *31*(2), 04018362.

[16] Yu.A. Klimon., A state of the art composite rebar for the reinforcement concrete structures., 2010, Kyiv national university of construction and architecture, Ukraine.